Spatially Fed Array Optimization with Adaptive Templates

Álvaro F. Vaquero[1,2], Marcos R. Pino[1], Manuel Arrebola[1], Fernando Las-Heras[1]
[1] Dept. Electrical Engineering, Universidad de Oviedo, Gijón, Spain, {fernandezvalvaro, mpino, arrebola, flasheras}@uniovi.es
[2]Instituto de Telecomunicações, Instituto Superior Tecnico, Univ. Lisboa, Lisboa, Portugal

***Abstract*—This work presents two techniques for synthesizing Spatially Fed Array antennas within the framework of the Intersection Approach. The first technique introduces a methodology to address highly complex synthesis problems, particularly for optimizing antennas that require complex near-field shaped patterns. The second technique offers an acceleration of the gradient computation in optimization algorithms, reducing the computation times and making near-field synthesis more manageable. Both techniques are integrated within the Intersection Approach for the synthesis of a metalens. The presented example achieves a uniform near-field pattern over a relatively large area, starting from a focused near-field beam.**

***Index Terms*—Near field synthesis, Spatially Fed Array, Metalens optimization.**

I. Introduction

Wireless technology has become increasingly popular in various applications, such as Radio Frequency Identification (RFID), Wireless Power Transfer (WPT), Remote Sensing, among others. The advancements in communications systems, particularly the evolution of the current Fifth Generation (5G) of mobile communications, have significantly heightened the interest in wireless technology. The latest generation, known as 5G, as well as its successors *Beyond* 5G (B5G) and the future 6G, have driven the exploration of higher frequencies to achieve larger bandwidths and faster data-rate communications. Within this context, the sub-6 band, also referred to us as Frequency Range 1 (FR1), encompasses communication systems operating at frequencies below 6 GHz. However, one of the main challenges in future communication systems lies in the deployment of mm-Wave frequency bands. These systems are intended to operate within various bands ranging from 28 to 200 GHz, aiming to provide high-speed wireless access in cellular networks [1]. However, deploying communication systems in the Ka-band or higher frequencies poses significant obstacles in terms of signal propagation. Specifically, path losses and sensitivity to physical barriers are notably increased compared to FR1. Overcoming these challenges requires a well-designed base station antenna system.

Antennas play a crucial role in adapting to the requirements imposed by new wireless applications, technologies, and deployment scenarios. It is essential to ensure efficient coverage, reliable radio links, and wireless connectivity through well-designed antennas. In indoor scenarios, the distance between the user and base station is relatively short, therefore, the devices are typically located in the radiative near field of the base station. These indoor scenarios deviate from the extensive coverage areas provided by external base stations and focus on smaller areas where devices are located. Moreover, indoor base stations can cover areas that are not served by external base stations, addressing "blind" or "dead" zones with poor or even null coverage [2]. Consequently, developing antennas with near-field-shaped beams, similar to far-field patterns, becomes a crucial factor in current and future communications systems [3].

A Spatially Fed Array (SFA) antenna is suitable choice for serving as an indoor base station. These antennas combine a primary feed with a phased array antenna, such as reflectarray, transmitarray, metalens or metasurface antenna. The primary feed eliminates the need for a feeding network to excite the elements, thereby improving radiation efficiency, especially at mm-Wave or higher frequency bands. Moreover, several studies have demonstrated that SFA antennas can generate complex-shaped patterns with stringent requirements for space communications [4].

While many published works have focused on synthesizing the far-field radiation of SFA antennas [5], [6], there have been limited examples addressing the synthesis of the near-field components. Some recent approaches utilize a multi-focus technique or iterative application of the direct and inverse Fast Fourier Transform (FFT) [7]. However, these methods have limitations in terms of the addressed geometries and pattern shapes. To overcome these limitations, a general approach based on the generalized Intersection Approach (gIA) for the near field has been proposed in [8]. The gIA offers an efficient way to generate complex-shaped beam patterns within the radiated near field of an SFA.

This work introduces the IA for synthesizing a SFA antenna with constraints on the magnitude of the near field to achieve a uniform-field distribution in a complex scenario. It also presents a novel strategy for addressing complex scenario requirements. The aim is to generate a complex near-field coverage area defined in a plane transverse and offset to the antenna aperture over several meters. The proposed procedure utilizes the electric field itself to define the template used in the synthesis, leading to intermediate solutions that facilitate the convergence of the gIA. The proposed method overcomes the need for confining the synthesis process to planes parallel to the antenna aperture. The procedure has shown successful results in challenging scenarios, producing a phase-shift distribution that radiates a well-shaped near-field pattern. To

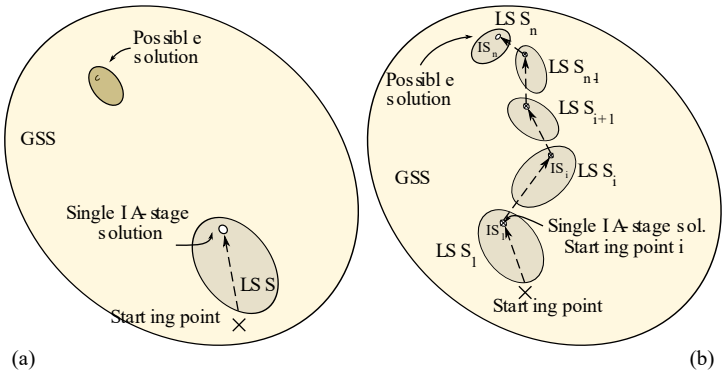

Figure 1. Sketch of the displacement of the Local Space Search using (a) conventional single-stage strategy and (b) proposed F2M adaptive process.

validate the approach, a prototype is designed, and manufactured reaching a high agreement with both synthesis and full-wave simulations. Moreover, this technique is introduced together with finite differences to accelerate the computation of the gradient of local search algorithms used in the generalized Intersection Approach. The approach is based on two key principles. First, in SFA or more generally in array synthesis, each element is analyzed independently, without considering the influence of other elements. This allows for a more efficient computation process. Second, the linearity of Maxwell's equations establishes a linear relationship between the field in the antenna aperture and the radiated field, whether it is in the near or far field. As a result, when evaluating each derivative, only the specific contribution of the element under consideration is considered, which helps to save computing time. The combination of both techniques reaches an efficient and fast technique based on the Intersection Approach framework for the synthesis of SFA antennas with near-field constraints.

II. Adaptive Field-to-Mask (F2M) Procedure to Enhance the Convergence

The IA is a powerful technique in the synthesis of SFA or conventional array antennas. The IA has been typically used for the synthesis of the co-polar component of the near- and far-field radiated by such antennas. However, the IA is an algorithm of local optimization, an as such, the convergence and attainment of the desired solution are significantly influenced by the starting point (SP) and the sought specifications (typically related to the radiation pattern).

Figure 1(a) shows the Global Search Space (GSS), which includes the solution or set of solutions that meet the desired specifications. It also displays the Local Search Space (LSS), where the IA will seek a solution, regardless of whether the desired solution is contained within it or not. For cases with stringent requirements, such as space or terrestrial communications, the set of possible solutions within the GSS can be very limited. Therefore, if the SP is not chosen appropriately, it is highly possible that the IA will converge to a local minimum within the LSS without reaching the desired solution. As Figure 1 shows, the desired solution is far away from the starting point, therefore, it is not contained within the LSS. On the other hand, the definition of templates (based on the desired specifications) has a significant impact on the synthesis of the near-field components, where uniform field distributions are typically sought, taking into account the inherent effects of electromagnetic waves. For instance, when seeking a certain field distribution for a specific scenario, factors such as the geometry and propagation effects need to be considered. This can lead to complex field patterns that may involve the use of templates that are challenging to define, which can hinder the IA's convergence to a valid solution.

A strategy to enhance convergence and minimize the aforementioned effects is to employ a multi-stage synthesis process. Starting from a known SP (typically an analytical approach), templates related to the desired specifications but more relaxed are defined. This reduces the risk in SP selection and facilitates the attainment of an intermediate solution (IS_1), which does not fulfill the desired requirements but is contained within LSS_1 and reachable by the IA. Subsequently, during the intermediate stages, the templates become increasingly strict and closer to the final desired solution. By adjusting the templates at each stage i, the LSS of that stage (LSS_i) is modified to include a solution for the specifications of that stage. The changes in the template should be a combination of the final desired specifications and the intermediate solution obtained in the previous stage (IS_{i-1}), so that IS_{i-1} is used as the SP in the stage i, as it is depicted in Figure 1(b).

To define the initial set of intermediate specifications (or intermediate masks, IM_1), the SP in terms of the radiated field and the geometry of the desired final specifications are used. In this case, the LSS_1 will be defined as the search space where the IA will search for the intermediate solution, IS_1. In a subsequent synthesis, IS_1 will act as the SP for this new stage, and a new set of intermediate masks, IM_2, will be defined, resulting in a new LSS_2 where IS_2 resides. This process will be repeated in successive synthesis stages, with IM_i, LSS_i, and IS_i progressively evolving to reach LSS_n. This final LSS_n contains the desired final solution.

Ideally, this strategy guides the algorithm towards the desired solution from a given SP, regardless of whether it is close or not. However, the selection of intermediate specifications has a significant impact on guiding the IA and generating the LSS_i, which can potentially affect the

algorithm's convergence. Specifications are typically expressed in terms of masks or templates, defined based on the desired radiation parameters. In the case of far-field synthesis, these are often obtained considering the desired gain, side lobe levels (SLL), shaped pattern, or other factors.

At each intermediate stage, and therefore for the intermediate specifications, templates/masks are defined taking into account both the desired final solution and the field distribution obtained in the previous stage $i-1$. In this way, after multiple concatenated syntheses, with the corresponding definition of intermediate specifications, an LSS is reached that contains the desired solution, resulting in an output that meets the desired specifications.

III. Differential Contributions to Speed Up the Intersection Approach

Unlike most optimization algorithms, IA does not aim to minimize a cost function. Instead, it seeks the intersection of two sets or, in case of unattainability, minimizes the distance between them using the method of alternate projections. Two sets are defined: the set $\mathcal{R}$, which encompasses all fields that can be radiated by the antenna, and the set $\mathcal{M}$, which contains all field that meet the desired specifications. To project a point from $\mathcal{R}$ onto set $\mathcal{M}$, the forward projector is defined, while projecting a point from $\mathcal{M}$ onto $\mathcal{R}$ is defined as the backward projector [9].

The forward projector is typically defined to ensure that the radiated field satisfies the following condition:

$$G_{lwr}(\boldsymbol{r}) \leq |\widetilde{\boldsymbol{E}}^{i}_{rad}(\boldsymbol{r})| \leq G_{upr}(\boldsymbol{r}) \tag{1}$$

where G_{lwr} and G_{upr} are the lower and upper templates, respectively; $\widetilde{\boldsymbol{E}}^{i}_{rad}$ is the radiated field at the ith iteration of the IA and $\boldsymbol{r}$ is the point of observation wherein the field is computed.

In the case of the backward projector, the classical implementation relies on direct/inverse operators, such as the Fast Fourier Transform (FFT) and its inverse (iFFT). However, this implementation has certain disadvantages. Firstly, using FFT allows imposing conditions only on the radiated field in planes parallel to the aperture, limiting its applicability. Secondly, an issue of local optimizers is the presence of local minima, also known as traps. In the case of IA, these traps are typically associated with the number of degrees of freedom used (or optimization variables) and the non-convexity of the defined sets. Non-convexity can be avoided by working with radiated intensity instead of the radiated field, leading to (2) instead of (1). Now, direct/inverse operators can no longer be used, and an alternative method for defining the backward projector is required.

$$G^2_{lwr}(\boldsymbol{r}) \leq \left|\widetilde{\boldsymbol{E}}^{i}_{rad}(\boldsymbol{r})\right|^2 \leq G^2_{upr}(\boldsymbol{r}) \tag{2}$$

One alternative is to use a generalized version of IA, where a functional d is defined to evaluate the distance from an element of $\mathcal{M}$ to an element of $\mathcal{R}$. This allows the use of an optimization algorithm to minimize d (as it becomes a cost function) and implement the backward projector in this manner [10]. In our case, the Levenberg-Marquardt algorithm (LMA) is used to minimize d.

One of the main disadvantages of this implementation is that it tends to be less efficient compared to using FFT/iFFT. In particular, one of the most time-consuming operations on the LMA is the computation of the gradient, which is defined as (3) for a multidimensional scalar cost function.

$$\nabla d(\Omega, \bar{\phi}) = \left(\frac{\partial d(\boldsymbol{\Omega}, \bar{\phi})}{\partial \phi^1}, \cdots, \frac{\partial d(\boldsymbol{\Omega}, \bar{\phi})}{\partial \phi^i}, \cdots, \frac{\partial d(\boldsymbol{\Omega}, \bar{\phi})}{\partial \phi^m}\right) \tag{3}$$

where an element of $\boldsymbol{\Omega}$ is an observation point defined as $\boldsymbol{\Omega}_t = (x_t, y_t, z_t)$ and $\bar{\phi} \in (\phi^1, \cdots, \phi^i, \cdots, \phi^m)$ is a vector whose elements are the optimization variables.

In the case where an analytical expression is not available, the derivative can be calculated using finite difference. For the case of the backward lateral difference, the derivative is computed using (4) (the dependence on $\boldsymbol{\Omega}$ has been removed to simplify the notation).

$$\frac{\partial d(\bar{\phi})}{\partial \phi^i} = \frac{d(\bar{\phi}) - d(\bar{\phi} - h\delta_{ij})}{h} + \mathcal{O} \tag{4}$$

where h is a small positive scalar and δ_{ij} is the Kronecker delta, which takes the value of 1 when $i = j$ and 0 otherwise. Therefore $(\bar{\phi} - h\delta_{ij})$ is defined as :

$$(\bar{\phi} - h\delta_{ij}) = (\phi^1, \cdots, \phi^i - h, \cdots, \phi^m) \tag{5}$$

Despite the high computational cost of computing the gradient, it can be accelerated using the technique of differential contributions. To do this, two conditions must be met: that the modification of one variable does not affect the others, and that the process of calculating the cost function is linear. The first condition is satisfied when the analysis of an element of the SFA is independent of the others, as is the case in local periodicity. The second condition requires that the calculation of the gradient, in whole or in part, be linear. Typically, local optimization algorithms make use of nonlinear cost function, breaking this condition. However, the linearity of Maxwell's equations can be leveraged. In particular, the relationship between the tangential field on the aperture and the radiated field is linear, which allows for the use of differential contributions to speed up the gradient calculation.

From (5), it can be deduced that the residue $d(\bar{\phi})$ is common to all derivatives in (4) and thus only needs to be calculated once. On the other hand, $d(\bar{\phi} - h\hat{e}_i)$ depends on the variable ϕ^m, and is computed in each derivative.

If we consider the condition of local periodicity, modifying a single element (or variable) of the SFA does not affect the rest. Therefore, the perturbated field can be calculated by extracting the original contribution of the unaffected element and adding the contribution generated by the perturbated element. Consequently, the residue $d(\bar{\phi} - h\hat{e}_i)$ can be computed as

$$d(\bar{\phi} - h\hat{e}_i) = \left[|\widetilde{\boldsymbol{E}}_{rad}(\bar{\phi})|^2 - \left(|\widetilde{\boldsymbol{E}}^{i+1}_{rad}(\bar{\phi}) + \Delta\widetilde{\boldsymbol{E}}^{i+1}_{rad}(\bar{\phi}^m)\right)^2\right] \tag{6}$$

where $\Delta\widetilde{\boldsymbol{E}}^{i+1}_{rad}(\bar{\phi}^m)$ is the differential contribution of the radiated field by the element/variable m, defined as

$$\Delta\widetilde{\boldsymbol{E}}^{i+1}_{rad}(\bar{\phi}^m) = \boldsymbol{E}^{i+1}_{rad}(\phi^m - h) - \boldsymbol{E}^{i+1}_{rad}(\phi^m) \tag{7}$$

Therefore, in the calculation of a derivative, it is only necessary to compute the differential contribution of the perturbed element, which accelerates the overall gradient calculation in each iteration of the LMA.

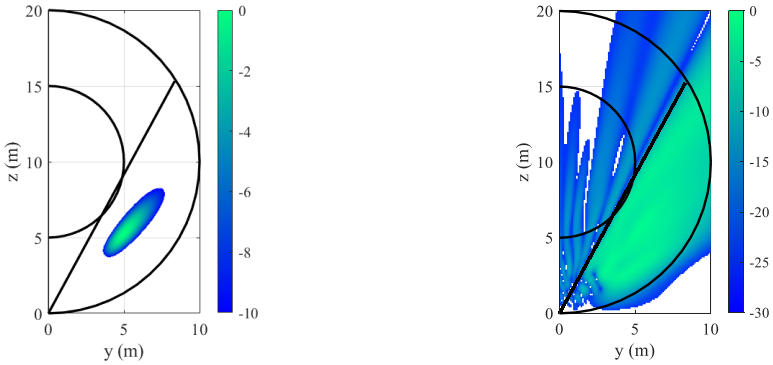

Figure 2. Amplitude (dB) of the radiated near field (a) before and (b) after the synthesis using the F2M approach. The field is normalized to its maximum.

IV. Experimental Validation

Both techniques have been used to design a metalens antenna for generating indoor coverage in complex scenarios. In particular, a metalens composed of 1936 elements with periodicity $2.5 \times 2.5\ \text{mm}^2$ and a F/D of 0.45 has been designed. The antenna operates at 39 GHz and is fed by a 15 dBi-gain horn antenna that generates a 20 dB taper over the surface of the antenna. The coverage will be generated in a plane perpendicular to the aperture at a height of 1.5 m, aiming to cover an area within a circular ring with radius of 5 and 10 m, in a near-field range of approximately 14 m.The design of the metalens has been accomplished using a generalized IA-based Phase-Only Synthesis, starting with a near-field focus approach as SP (obtained analytically).

Figure 3 shows the near-field distribution before and after the synthesis. A smooth field distribution with minimal ripple has been achieved over the desired surface. When analyzing the field distribution of the SP, it can be seen that the difference in relative levels across the entire area exceeds 30 dB, whereas after synthesis, it is reduced to just 5 dB. It should be noted that achieving such a reduction is highly complex, as it involves homogenizing the field over a range of nearly 14 m in length.

These results have been made possible through the use of the F2M and differential contributions. Additionally, it is worthy to note that the SP is significantly distant from the desired and achieved endpoint.

V. Conclusions

This work introduces two techniques for optimizing spatially fed array antennas using the Intersection Approach framework. In particular, one technique has been introduced to enhance the convergence of the IA and address near-field synthesis with highly complex requirements. The second technique accelerates the computation of the gradient in local optimization algorithms, making it possible to tackle computationally expensive problems such as near-field synthesis. Both techniques have been combined to synthesize a metalens with a near-field pattern designed for coverage in a complex indoor scenario. Simulations have demonstrated the evolution of the near-field pattern, going from a focused beam to a relatively complex field distribution. More experimental results will be shown in the presentation.

Acknowledgment

This work was supported in part by MCIN/AEI/10.13039/501100011033 under grants PID2020-114172RB-C21 and TED2021-130650B-C22, cofounded by UE (European Union) "NextGenerationEU"/PRTR; by Gobierno del Principado de Asturias under grant AYUD/2021/51706; and by the Spanish Ministry of Universities and European Union (NextGenerationEU/PRTR) under grant MU-21-UP2021-03071895621J.

References

[1] T. S. Rappaport, Y. Xing, G. R. MacCartney, A. F. Molisch, E. Mellios and J. Zhang, "Overview of Millimeter Wave Communications for Fifth-Generation (5G) Wireless Networks With Focus on Propagation Models," *IEEE Trans. Antennas Propag.*, vol. 65, no. 12, pp. 6213-6230, Dec. 2017.

[2] A. Mudonhi, M. Lotti, A. Clemente, R. D'Errico and C. Oestges, "RIS enbaled mmWave Channel Sounding Based on Electronically Reconfigurable Transmitarrays," *2021 15th European Conference on Antennas and Propagation (EuCAP)*, 2021, pp. 1-5.

[3] Á. F. Vaquero, M. R. Pino, and M. Arrebola, "Dual-Polarized Shaped-Beam Transmitarray to Obtain Multizone Coverage for 5G Indoor Communications," *IEEE Antennas Wirel. Propag. Lett.*, vol. 21, no. 4, pp. 730-734, Apr. 2022.

[4] J. A. Encinar *et al.*, "Dual-Polarization Dual-Coverage Reflectarray for Space Applications," *IEEE Trans. Antennas Propag.*, vol. 54, no. 10, pp. 2827-2837, Oct. 2006.

[5] M. Zhou *et al.*, "Direct Optimization of Printed Reflectarrays for Contoured Beam Satellite Antenna Applications," *IEEE Trans. Antennas Propag.*, vol. 61, no. 4, pp. 1995-2004, Apr. 2013.

[6] C. C. Cruz, C. A. Fernandes, S. A. Matos, and J. R. Costa, "Synthesis of Shaped-Beam Radiation Patterns at Millimeter-Waves using Transmit Arrays," *IEEE Trans. Antennas Propag.*, vol. 66, no. 8, pp. 4017-4024, Aug. 2018.

[7] S. M. Feito, F. Foglia Manzillo, A. Clemente, and M. Arrebola, "Near-Field Shaped Transmitarray Antennas: Synthesis and Impact of Phase Quantization," *2023 17th European Conference on Antennas and Propagation (EuCAP)*, Florence, Italy, 2023, pp. 1-5.

[8] Á. F. Vaquero *et al.*, "Demonstration of a Reflectarray With Near-Field Amplitude and Phase Constratints as Compact Antenna Test Range Probe for 5G New Radio Devices," *IEEE Trans. Antennas Propag.*, vol. 69, no. 5, pp. 2715-2726, May 2021.

[9] O. M. Bucci, G. D'Elia, G. Mazzarella, and G. Panariello, "Antenna pattern synthesis: a new general approach," *Proc. IEEE*, vol. 82, no. 3, pp. 358-371, Mar. 1994.

[10] O. M. Bucci, G. D'Elia, G. Romito, "Power synthesis of conformal arrays by a generalised projection method," *IEE Proc. Microw. Antennas Propag.*, vol. 142, no. 6, pp. 467-471, Dec. 1995.